NCX1 coupled with TRPC1 to promote gastric cancer via Ca^{2+}/AKT/β-catenin pathway

Hui Dong (h2dong@ucsd.edu)
University of California
Hanxing Wan
Nannan Gao
Wei Lu
Cheng Lu
Jun Chen
Yimin Wang

Article

Keywords: NCX1, TRPC1 channels, gastric cancer, helicobacter pylori, virulence factors

Posted Date: May 12th, 2022

DOI: https://doi.org/10.21203/rs.3.rs-1640004/v1

Version of Record: A version of this preprint was published at Oncogene on July 26th, 2022. See the published version at https://doi.org/10.1038/s41388-022-02412-9.

Abstract

Plasma membrane Na^+/Ca^{2+} exchanger 1 (NCX1) is a bidirectional ion transporter to operate in Ca^{2+} entry and exit modes, and TRPC1 is Ca^{2+}-permeable membrane channels. Both play critical roles in maintaining cytosolic free Ca^{2+} ($[Ca^{2+}]_{cyt}$) homeostasis in mammalian cells. Although either TRPC1 channels or Ca^{2+} entry mode of NCX1 is implicated in several human tumorigenesis, it has not been explored for a coordination of NCX1 and TRPC1 to involve in the pathogenesis of *H. pylori*-associated gastric cancer (GC). The protein expression of NCX1 was significantly enhanced in human GC specimens, which correlated with tumor progression and poor survival in GC patients. TRPC1 and NCX1 proteins were parallelly enhanced，co-localized and bound in human GC cells. By a functional coupling, TRPC1 drives NCX1 to its Ca^{2+} entry mode to raise $[Ca^{2+}]_{cyt}$ in GC cells. Moreover, $CaCl_2$, *H. pylori* and their virulence factors all enhanced expressions and activities of NCX1 and TRPC1, and evoked aberrant Ca^{2+} entry to promote proliferation, migration, and invasion of GC cells through AKT/b-catenin pathway. Tumor growth and metastasis also depended on the enhanced expression of NCX1 in subcutaneously xenografted GC model of nude mice. Overall, our findings indicate that TRPC1/NCX1 coupling may promote *H. pylori*-associated GC through the Ca^{2+}/AKT/b-catenin pathway. Since Ca^{2+} exit mode and Ca^{2+} entry mode of NCX1 play different roles under mostly physiological and pathological conditions respectively, we propose that targeting TRPC1/NCX1 coupling could be a novel strategy for selectively blocking Ca^{2+} entry mode to potentially treat digestive cancer.

Introduction

Since gastric cancer (GC), one of leading cause of cancer-related death worldwide, is difficult to cure once it metastasizes [1], it is urgent to explore early diagnostic markers and novel therapeutic targets responsible for GC. Helicobacter pylori (*Hp*) infection in the stomach is a well-known risk factor for GC and ammonia/ammonium is the major *Hp* virulence factors [2], but their pathogenesis in GC is still obscure. Therefore, it is critical to elucidate molecular pathogenesis of *Hp*-associated GC. Cytosolic free Ca^{2+} ($[Ca^{2+}]_{cyt}$) is a pivotal second messenger in eukaryotic cells to maintain critical cellular processes, including the energetic metabolism, cell signaling, and cell motility, *etc* [3–5]. Numerous findings indicate that aberrant $[Ca^{2+}]_{cyt}$ signaling is involved in GC, though the occurrence and progression of cancer are complex [6–8]. Since membrane Ca^{2+}-permeable channels and transporters play important roles in the regulation of $[Ca^{2+}]_{cyt}$, their aberrant expression and function are associated with GC development [9–11].

The Na^+/Ca^{2+} exchanger (NCX) is a bidirectional transporter that induces Ca^{2+} efflux (when operating as Ca^{2+} exit mode), or Ca^{2+} influx (when operating as Ca^{2+} entry mode), depending on the electrochemical gradient of the substrate ions and membrane potential [12]. Three different protein isoforms of NCX were described [12], NCX1 has a broad expression in multiple organs, including the heart, kidney, and gastrointestinal (GI) tract, *etc*, whereas NCX2 is found in the brain only but NCX3 in both brain and skeletal muscle [13, 14]. NCX has been investigated predominately in human brain, heart and kidney, and

the therapeutic potentials of its modulators are also emerging for the related disease. However, the molecular and functional aspects of NCX in GI organ, especially in GI cancer are scarce although it is likely involved in aberrant $[Ca^{2+}]_{cyt}$ homeostasis in other cancer cells [15]. It has been shown that NCX1 is expressed in the rat small intestine [16]. In the stomach, although the expression and function of NCX were reported in human gastric smooth muscle cells and myofibroblasts [17], they have not been explored in gastric epithelium. Furthermore, emerging evidence suggests a pathogenesis role of NCX glioblastoma, melanoma, and ovary carcinoma [15]. We and others also revealed a role of NCX1 in esophageal squamous cell carcinoma and hepatocellular carcinoma [18, 19], but its role in the adenocarcinoma of GI tract have not been explored yet.

Transient receptor potential canonical (TRPC) channels as Ca^{2+}-permeable channels are ubiquitously expressed in various cell types, including GI epithelial cells to regulate $[Ca^{2+}]_{cyt}$ homeostasis [20]. Among seven members of TRPC subfamilies, TRPC1 is crucial for metastasis by epithelial-mesenchymal transition (EMT) activation in several kinds of tumors [21, 22]. We reported previously that TGF-β–induced Ca^{2+} entry via TRPC1/NCX1 coupling to modulate Ca^{2+}-mediated motility of human pancreatic duct cells [23]. Although TRPC1 is highly expressed in human GC to likely promote GC progression [24], it is currently unknown whether TRPC1 couples with NCX1 to contribute to this process. Therefore, in the present study, we sought to investigate if NCX1 and TRPC1 are involved in GC and, if so, what the underlying molecular mechanisms are.

Results

Enhanced NCX1 expression in human primary GC tissues

Due to the lack of information on NCX1 expression in the stomach of normal subjects and GC patients, we first collected human primary GC tissues and corresponding adjacent tissues to compare NCX1 expression. By applying Western blotting analysis, total 55 pairs of fresh gastric tissues obtained from GC patients were compared. As shown in Fig. 1, 36 pairs had higher NCX1 protein expression in human GC tissues than in adjacent tissues (Fig. 1A), accounting for 65% (Fig. 1D). In contrast, 13 pairs had lower NCX1 expression in GC tissues (Fig. 1B), accounting for 24% (Fig. 1D). However, 6 pairs had no difference (Fig. 1C), accounting for 11% (Fig. 1D). Therefore, NCX1 protein expression was enhanced in human primary GC tissues.

Second, immunohistochemstry study was applied to human gastric tissues from 80 GC patients. Among these patients, their average age was 64 years old, 76% was male, 56% was diagnosed with advanced-stage (III/IV), and 73% had lymphatic metastasis (Supplementary table 1). As shown in Fig. 1E and F, the protein expression of NCX1 was markedly enhanced in GC tissues compared to their adjacent tissues, but staining was not detected in the negative control, indicating its specific staining to NCX1 proteins. Third, the association between NCX1 expression and clinicopathologic parameters of GC progression was subsequently analyzed. As shown in Fig. 1G-I, the up-regulation of NCX1 expression was correlated with

the advanced clinical stage, the large tumor size, lymphatic metastasis. Furthermore, Kaplan-Meier analysis showed that the GC patients with high NCX1 expression had a poor prognosis, but those with low expression had a better prognosis (Fig. 1J). Altogether, the close association between NCX1 expression and clinicopathologic parameters strongly suggests an oncogenic role for NCX1 in human GC.

Co-localization and binding of the enhanced NCX1 and TRPC1 in human GC cells

Since enhanced expression of TRPC1 was closely related to GC prognosis and it exacerbated EMT in GC [24, 25], we first compared the expression of both TRPC1 and NCX1 proteins between normal human gastric epithelial cells (GES1) and five human GC cell lines (MKN45, SGC7901, AGS, BGC823, and SNU216). As shown in Fig. 1K, the expression level of NCX1 proteins was markedly enhanced in all GC cells compared to the GES1 cells. Similarly, the expression level of TRPC1 proteins was also markedly enhanced in all GC cells (Fig. 1L), suggesting both NCX1 and TRPC1 are expressed parallelly. Second, we performed immunofluorescence analysis to further study the expression and localization of NCX1 and TRPC1 proteins in human GC cells. As shown in Fig. 1M, both NCX1 and TRPC1 proteins were confirmed to express parallelly in three GC cells, but non-specific staining was undetected in the negative control without primary antibody. Moreover, both NCX1 and TRPC1 proteins were predominately expressed and co-localized on the plasma membrane of GC cells (Fig. 1M). Finally, our coimmunoprecipitation study clearly showed the binding of NCX1 and TRPC1 in GC cells (Fig. 1N-Q). Therefore, the expression of NCX1 and TRPC1 is not only up-regulated but also co-localized and bound on the plasma membrane of human GC cells.

NCX1 activation promotes proliferation, migration and invasion of human GC cells in vitro

To examine the role of NCX1 in GC, we first determined the cell proliferation of 3 human GC cell lines commonly used in the literature (MKN45, AGS and SGC7901). The varying concentrations of $CaCl_2$ were applied to stimulate the Ca^{2+} entry mode of NCX1 since no selective activators of NCX1 are commercially available so far [26]. $CaCl_2$ at the concentrations of 0.1-2 mM, dose-dependently promoted proliferation of all GC cells (Fig. 2A, D, G), which was attenuated by KB-R7943, a selective inhibitor for the Ca^{2+} entry mode of NCX1 (Fig. 2B, E, H). The concentrations of KB-R7943 were chosen in the light of the different sensitivity of GC cell proliferation to the drug (Supplementary Fig. 1A, B, C, D). Similarly, $CaCl_2$ dose-dependently promoted proliferation of CHO cells with NCX1 overexpression (CHO-NCX1) (Fig. 2P), which was attenuated by KB-R7943 (Fig. 2Q). However, $CaCl_2$ could not influence proliferation of CHO cells without NCX1 overexpression (CHO-K1) (Fig. 2R) and GES1 cells without NCX1 expression (Fig. 2T). Therefore, $CaCl_2$ promotes GC cell proliferation most likely via activating the Ca^{2+} entry mode of NCX1.

Although NCX1 enhanced migration and invasion of hepatocellular carcinoma [19], its contribution to GC progression is unknown. Second, we examined the role of NCX1 in migration and invasion of human GC cells. Cell scratch test showed that $CaCl_2$ promoted migration of MKN45 and AGS cells, which was attenuated by KB-R7943 (Supplementary Fig. 2A, B). Moreover, transwell assays showed that $CaCl_2$

promoted migration (Supplementary Fig. 2C, D) and invasion (Fig. 2C, F, I) of MKN45, AGS and SGC7901 cells, which were attenuated by KB-R7943 (Supplementary Fig. 2C, D and Fig. 2C, F, I). Finally, after shNCX1 was applied to successfully knock down the protein expression of NCX1 in GC cells (Fig. 3A, B, C), $CaCl_2$-induced cell proliferation (Fig. 3D, F, H), migration (Supplementary Fig. 3A, B, C) and invasion (Fig. 3E, G, I) were all inhibited. Taken together, NCX1 plays a critical role in GC cell proliferation, migration and invasion.

Hp virulence factor promotes GC cell proliferation, migration and invasion via NCX1 activation

Since *H. pylori* infection is a pivotal risk factor for tumorigenesis of GC and ammonia/ammonium is a major *H. pylori* virulence factor, NH_4Cl was applied to the present study as a well-known ammonia/ammonium [2]. As shown in Fig. 2, like $CaCl_2$, NH_4Cl dose-dependently (0.1-2 mM) promotes proliferation of MKN45, AGS and SGC7901 cells (Fig. 2J, L, N), which was attenuated by KB-R7943 (Fig. 2K, M, O). However, NH_4Cl did not affect proliferation of CHO-K1 (Fig. 2S) and GES1 cells (Fig. 2U). Similarly, NH_4Cl-induced cell proliferation (Fig. 3J, L, N), migration (Supplementary Fig. 3D, E, F) and invasion (Fig. 3K, M, O) were all inhibited by knockdown of NCX1 protein expression in GC cells. Therefore, *Hp* virulence factor promotes GC cell proliferation, migration and invasion via NCX1 activation.

$CaCl_2$, Hp and their virulence factors enhance NCX1 expression in GC cells

After demonstrating the promoted action of $CaCl_2$ and *Hp* virulence factors on cell proliferation, migration and invasion, we also examined if they affect NCX1 expression of GC cells. Indeed, $CaCl_2$ enhanced NCX1 expression in MKN45, AGS and SGC7901 cells (Fig. 4A, G, M), which was attenuated by either KB-R7943 (Fig. 4B, H, N) or shNCX1 (Fig. 4C, I, O). Moreover, *H. pylori* virulence factor NH_4Cl enhanced NCX1 expression in GC cells (Fig. 4D, J, P), which were attenuated by either KB-R7943 (Fig. 4E, K, Q) or shNCX1 (Fig. 4F, L, R). Similarly, another *H. pylori* virulence factor lipopolysaccharide (LPS) enhanced NCX1 expression in GC cells (Fig. 4S, T, U). Finally, *H. pylori* per se co-culture with MKN45 and AGS cells for 24 h also enhanced NCX1 expression (Fig. 4V, W). However, $CaCl_2$, NH_4Cl, LPS and *H. pylori* all did not affect NCX1 expression in GES1 cells as negative control (Supplementary Fig. 4A, B, C, D). Taken together, these data strongly suggest that like $CaCl_2$, *H. pylori* and their virulence factors promote GC through enhancing NCX1 expression.

NCX1 coordinates with TRPC1 to promote GC cell proliferation and migration

TRPC family is a potential partner for the Ca^{2+} entry mode of NCX1 [27]. Among them, TRPC1 is highly expressed in human GC to play an oncogenic role in GC progression [24]. We therefore focused on a possible coupling of TRPC1 and NCX1 in GC development. As shown in Fig. 5, $CaCl_2$-induced proliferation and migration of MKN45, AGS and SGC7901 GC cells were attenuated by either KB-R7943 or a TRPC1 blocker SKF96365 (its concentrations were also chosen in the light of the different sensitivity of GC cell

proliferation to the drug (Supplementary Fig. 1E, F, G)); however, $CaCl_2$-induced cell proliferation and migration were further attenuated by a combination of the selective inhibitors for both NCX1 and TRPC1 (Fig. 5A-C, G-I). Similarly, $CaCl_2$-induced cell proliferation and migration were further attenuated by a combination of shNCX1 plus SKF96365 (Fig. 5D-F, J-L). Taken together, these data suggest that NCX1 coordinate with TRPC1 to promote GC cell proliferation and migration.

Hp **virulence factor could stimulate TRPC1 channels to trigger Ca^{2+} entry mode of NCX1 in GC cells**

We next applied single cell live Ca^{2+} imaging to determine if NCX1 operates in Ca^{2+} entry mode to induce $[Ca^{2+}]_{cyt}$ increase in GC cells. First, extracellular 0 Na^+ that triggers Ca^{2+} entry mode of NCX1 could significantly induce $[Ca^{2+}]_{cyt}$ signaling in Ca^{2+}-containing solutions but not in Ca^{2+}-free solutions (Fig. 6A). Second, 0 Na^+-induced $[Ca^{2+}]_{cyt}$ signaling in Ca^{2+}-containing solutions could be abolished by KB-R7943 (Fig. 6B). Third, 0 Na^+ also markedly increased $[Ca^{2+}]_{cyt}$ signaling in CHO-NCX1 cells with NCX1 overexpression (Fig. 6G, I, J), but not in CHO-K1 without NCX1 overexpression (Fig. 6H, I, J). These data strongly support NCX1 operates in Ca^{2+} entry mode in GC cells like in CHO-NCX1 cells. We further examined if *Hp* virulence factor NH_4Cl and the local acidic micro-environment in *Hp* infection-induced chronic inflammation and tumorigenesis could stimulate NCX1 activity. Like 0 Na^+, NH_4Cl and acid (pH4.5) indeed had similar stimulation on Ca^{2+} entry mode of NCX1 in SGC7901 cells (Fig. 6C, D, E, F).

We further examined TRPC1/NCX1 coupling-mediated Ca^{2+} signaling in GC cells since NCX1-induced Ca^{2+} entry requires the electrochemical gradient of the substrate ions and membrane potential, depending on Na^+ entry via TRPC channels [27]. After shTRPC1 successfully knocked down TRPC1 expression in GC cells (Fig. 6N, R), both 0 Na^+ and NH_4Cl-induced Ca^{2+} signaling was almost abolished (Fig. 6K-M, O-Q). These data verify that *Hp* virulence factor could stimulate TRPC1/NCX1 coupling to induce Ca^{2+} signaling in GC cells.

NCX1 activation promotes GC through AKT/β-catenin pathway

We next elucidated the oncogenic mechanisms of NCX1 in GC. Since previous studies revealed the important role of AKT/β-catenin pathway in GC [28] and colorectal cancer [29], and aberrant $[Ca^{2+}]_{cyt}$ promoted GC through AKT/β-catenin pathway [11], we therefore examined their role in NCX1-promoted GC. First, after NCX1 was activated by $CaCl_2$, both AKT phosphorylation (Ser473) and β-catenin phosphorylation (Ser675) were increased in MKN45 and AGS cells (Fig. 7A-B, E-F, I-J, M-N). Second, the $CaCl_2$-induced phosphorylation of AKT and β-catenin in MKN45 and AGS cells were attenuated by either KB-R7943 (Fig. 7A-B, E-F) or NCX1 knockdown (Fig. 7I-J, M-N). Third, NH_4Cl also increased AKT phosphorylation (Ser473) and β-catenin phosphorylation (Ser675) in MKN45 and AGS cells (Fig. 7C-D, G-H, K-L, O-P), which were attenuated by KB-R7943 (Fig. 7C-D, G-H) and NCX1 knockdown (Fig. 7K-L, O-P).

Therefore, both $CaCl_2$- and NH_4Cl-induced NCX1 activation could stimulate phosphorylation of AKT and β-catenin in GC cells.

NCX1 couples with TRPC1 to promote GC through AKT pathway

Since NCX1 often coupled with TRPC1 to function [27], we investigated whether TRPC1 channels are involved in NCX1-mediated AKT phosphorylation. Western blotting analysis exhibited that after $CaCl_2$ induced AKT phosphorylation in MKN45 and SGC-7901 cells, either NCX1 inhibitor KB-R7943 or TRPC1 inhibitor SKF96365 significantly attenuated the $CaCl_2$-induced AKT phosphorylation; however, a combination of them further attenuated $CaCl_2$-induced AKT phosphorylation (Fig. 8A, D). Moreover, either a combination of shNCX1 and SKF96365 (Fig. 8B, E) or a combination of shTRPC1 and KB-R7943 (Fig. 8C, F) further attenuated the $CaCl_2$-induced AKT phosphorylation. These data verify a TRPC1 and NCX1 coupling enhances AKT phosphorylation in GC cells.

NCX1 activation enhances GC growth and metastasis in vivo

We applied subcutaneously xenografted GC model of nude mice to further verify the oncogenic role of NCX1 in GC growth *in vivo*. NCX1 activation by $CaCl_2$ increased tumor weights (Fig. 8G), which was attenuated by KB-R7943 (Fig. 8H). Moreover, the knockdown of NCX1 in SGC-7901 cells by NCX1-shRNA lentiviruses markedly suppressed growth ability of GC cells after their implantation, leading to a significant decrease in tumor weights (Fig. 8I). Immunohistochemical analysis showed that the tumors derived from the implants pre-treated with NCX1-shRNA lentiviruses had lower expression of NCX1 and Ki67 than those pre-treated with control shRNA (Fig. 8K, L, M). Therefore, NCX1 stimulated GC growth *in vivo*.

We further applied abdominal transplantation tumor model of nude mice to verify the role of NCX1 in promoting GC metastasis *in vivo*. As shown in Fig. 8J, $CaCl_2$-induced GC cell metastasis was markedly suppressed by pretreatment with NCX1-shRNA lentiviruses. Compared to NC group, tumor numbers in the group pretreatment with NCX1-shRNA was decreased by about 50%. Therefore, NCX1 stimulated GC metastasis *in vivo* as well.

Discussion

In the present study, we demonstrate for the first time that NCX1 and TRPC1 are involved in GC development. Several lines of evidence suggest that NCX1 promotes human GC growth and metastasis by a novel coupling to TRPC1 channels. First, the expression of NCX1 and TRPC1 was enhanced in human primary GC tissues and most GC cell lines. Second, the enhanced NCX1 expression was closely correlated with poor progression and survival of GC patients. Third, NCX1 and TRPC1 were co-expressed in parallel, co-localized and bound on the membrane of GC cells. Forth, co-stimulation of NCX1 and TRPC1 with $CaCl_2$ and *Hp* virulence factors promoted proliferation, migration and invasion of GC cells *in*

vitro, and increased gastric tumor size, number and peritoneal dissemination *in vivo*. Fifth, by coupling with TRPC1, NCX1 operated in Ca^{2+} entry mode to promote GC through AKT/β-catenin signaling pathway.

NCX1 plays an important role in mediating $[Ca^{2+}]_{cyt}$ homeostasis in various types of human cells by exchanging Na^+ and Ca^{2+} in either direction depending on transmembrane electrochemical gradients [12]. Since NCX1 was investigated predominately in the cardiovascular, nervous, and renal systems [13], little is currently known about them in GI tract. There is one report on its expression in gastric smooth muscle to mediate normal motility [30]; however, so far no any reports are available on NCX1 in gastric epithelial cells. By focusing on the role of NCX1 in GI health and disease, we revealed previously that NCX1 plays a critical role not only physiologically in mediating lower esophageal sphincter relaxation[31] and intestinal epithelial ion transports [32], but also pathologically involving in GI inflammation and cancer [18, 33]. Disruption of $[Ca^{2+}]_{cyt}$ homeostasis induced by abnormal $[Ca^{2+}]_{cyt}$ regulators, especially the enhanced Ca^{2+} entry mode of NCX1, has been detected in several cancers, such as pancreatic cancer [33], breast cancer [34], glioblastoma [35], and melanoma [36], indicating its involvement in tumorigenesis. Although we have demonstrated the role of NCX1-mediated Ca^{2+} signaling in the development of esophageal cancer [18], pancreatic cancer [33] and hepatocellular carcinoma [19], the pathological roles of NCX1 in the stomach, especially in GC development remain totally unexplored. In the present study, we have verified that NCX1 expression was enhanced in human primary GC tissues and cells. Importantly, we demonstrate that the enhanced NCX1 expression in GC tissues was correlated with large tumor size, high histological grade, lymphatic metastasis, advanced clinical stage and poor prognosis; strongly suggesting NCX1 as a potential marker for GC prognosis.

We have provided further experimental data to support our notion that NCX1 plays a pivotal role in GC development. The activation of NCX1 with either calcium or *Hp* virulence factors promoted GC cell proliferation, invasion and metastasis both *in vitr*o and i*n vivo*, suggesting its critical oncogenic role in *Hp*-associated GC. Consistently, both selective blocker for the Ca^{2+} entry mode of NCX1 and its specific knockdown attenuated the oncogenic effects of NCX1. Therefore, NCX1 may play a general oncogenic role in GI cancer, such as in GC reported here and in esophageal cancer [18], pancreatic cancer [33] and hepatocellular carcinoma [19] reported previously. Moreover, several Ca^{2+}-permeable TRP channels may play different roles in GC development [9–11]. Although TRPC1 is highly expressed in human GC to likely promote GC progression [24], its association with NCX1 is unknown. Here we revealed not only enhanced TRPC1 expression but also its co-localization and binding with NCX1 in human GC cells. Importantly, TRPC1 activation promoted proliferation and migration of GC cells, which was attenuated by selective blockers of TRPC1 channels. Therefore, in parallel with NCX1, TRPC1 also plays an oncogenic role in GC.

Under physiological status, NCX1 primarily functions in Ca^{2+} exit mode to expel the increased $[Ca^{2+}]_{cyt}$; however, under some pathological conditions (such as in tumorigenesis), NCX1 could be switched to Ca^{2+} entry mode to allow sustained and aberrant Ca^{2+} entry [12]. Most reports have suggested TRPC as a potential partner for NCX mode switch in non-excitable cells (such as GC cells) [27]. Na^+ could enter

through the activated TRPC channels to raise $[Na^+]_{cyt}$ under the restricted plasma membrane space and induce membrane depolarization, switching NCX1 to its Ca^{2+} entry mode [27]. Indeed, in the present study we revealed a novel coupling of TRPC1 and the Ca^{2+} entry mode of NCX1 is involved in GC development because: 1) both NCX1 and TRPC1 play oncogenic roles in GC; 2) GC cell proliferation and migration could be further attenuated by a combination of selective blockers and specific knockdown of both NCX1 and TRPC1; 3) $CaCl_2$ and *Hp* virulence factors could stimulate functional coupling of TRPC1 and NCX1 to induce Ca^{2+} signaling in GC cells; 4) a protein-protein interaction of TRPC1 and NCX1 is verified in GC cells by our co-immunoprecipitation study. These findings are consistent with the previous reports on the NCX1 and TRPC coupling in pancreatic cancer cells [23] and hepatocellular carcinoma [19]. Therefore, due to a general existence of TRPC and NCX1 coupling in most digestive cancer cells, we propose this coupling would allow aberrant Ca^{2+} entry to promote digestive cancer.

It has been well documented that aberrant Ca^{2+} signaling is involved in the pathogenesis of several human disease, such as GC developed from chronic inflammation associated with gastric *Hp* infection [37]. Iimuro and colleagues found that dietary calcium enhanced *Hp*-induced gastritis in Mongolian gerbils [38]. In contrast, calcium channel blockers attenuated chemically induced gastritis and GC in rats [39, 40]. Consistently with our previous report on the oncogenic role of calcium in GC development [11], here we further reveal that $CaCl_2$ and *Hp* virulence factors could not only enhance the expression of NCX1 and TRPC1 but also activate them to promote GC development, strongly suggesting a critical role of TRPC1/NCX1-mediated aberrant Ca^{2+} signaling in *Hp*-associated GC.

TRPC1/NCX1-mediated Ca^{2+} signaling increased AKT and β-catenin phosphorylation in GC cells to promote cancer progression. In contrast, selective pharmacological inhibitors and specific knockdown of TRPC1/NCX1 resulted in marked decreases in $[Ca^{2+}]_{cyt}$, AKT and β-catenin phosphorylation and GC progression. Taken together, our results indicate that TRPC1/NCX1 coupling induces GC development through Ca^{2+}/AKT/β-catenin pathway (Fig. 8N), further confirming the pivotal role of this pathway in GC as in our previous report [11]. Therefore, our findings strongly suggest not only that aberrant Ca^{2+} entry could promote GC via Ca^{2+}/AKT/β-catenin pathway, but also that calcium supplement and *Hp* infection are likely synergistic risk factors for GC pathogenesis.

In conclusion, we demonstrate for the first time that TRPC1/NCX1 coupling promotes *Hp*-associated GC development. Mechanistically, TRPC1/NCX1 coupling-mediated aberrant Ca^{2+} entry activates the downstream AKT/β-catenin pathway to consequently promote GC progression. Although NCX and TRP channels represent a relatively new field of cancer research with most studies still in their infancy, they hold tremendous potential that has yet to be uncovered in the hopes of achieving major clinical breakthroughs in GC therapy. Particularly, due to a critical role of the Ca^{2+} exit mode of NCX1 under physiological status, targeting TRPC1/NCX1 coupling could be a novel strategy for selectively blocking the Ca^{2+} entry mode of NCX1 to potentially treat if not all solid cancers but at least digestive cancer.

Materials And Methods

Ethics statement and human tissue samples

All animal and clinical studies were approved by the Clinical Research Ethics Committee of the Qingdao University Medical College, Qingdao and Army Medical University (AMU), Chongqing, China. Fifty pairs of GC and adjacent tissues for Western blotting were collected from the surgical patients in Xinqiao Hospital of the AMU and all resected specimens were confirmed by pathological examination. Informed consent was obtained for all patients. All animal care and experimental procedures complied with the “Guide for the Care and Use of Laboratory Animals” published by the National Institutes of Health, USA. Animal studies are reported in compliance with the ARRIVE guidelines [41].

Cell culture

The human gastric normal epithelial mucosa cell line (GES1) and gastric cancer cell lines MKN45, SGC7901, AGS, MGC803, BGC823 and SNU216 were purchased from Chinese Academy of Sciences (Shanghai, China). The CHO cells with NCX1 overexpression and CHO-K1 cells without NCX1 overexpression were kindly provided by the University of California, San Diego, California, USA [31]. All cells were maintained in RPMI-1640, DMEM-HIGH GLUCOSE or F-12 medium (HyClone, USA) supplemented with 10% fetal bovine serum (HyClone, USA) and 1% penicillin/streptomycin (Invitrogen, USA) in a 37°C humidified atmosphere containing 5% CO_2.

Preparation and infection of lentiviruses

Lentiviruses were purchased from HANBIO (Shanghai, China). The sequences for NCX1 shRNA, TRPC1 shRNA and NC were as follows: shNCX1-1 (5'- GCTAGGATTCTGAAGGAACTT-3'), shNCX1-2 (5'- CATCTGGAGCTCGAGGAAATGTTAT-3'), shTRPC1 (5'- GCTAAGGATTTACTTGCACAA-3'), and NC shGFP (5'- TTCTCCGAACGTGTCACGTAA-3'). GC cells were infected with lentiviruses according to the protocol of the manufacturer.

Quantitative real-time PCR

Quantitative real-time PCR was performed as previously described [9, 10]. All samples were run in triplicate, and β-actin was used as an internal control. Primers were as follows: TRPC1: 5'-AGGATAGCCTCCGGCATTC-3', TRPC1: 3'-TTCCACCTCCACAAGACTTAGT-5'; β-actin: 5'-GGCATCCACGAAACTACCTT-3', β-actin: 3'-TCGTCCTCATACTGCTCAGGC – 5'. The siRNA plasmids of TRPC1 were purchased from RIBOBIO (Guangzhou, China). The transfection assays were performed according to the protocol of the manufacturer.

Western blotting

Western blotting was performed as previously described [9, 10]. The following antibodies are used: anti-NCX1, 1:1,000 (No. ab177952, Abcam, UK), anti-TRPC1, 1:200 (No. ACC-010, alomone labs, Israel), anti-β-catenin, 1:1000 (No. 8480, Cell Signaling Technology, USA), anti-phospho-β-catenin, 1:1000 (No. 9567,

Cell Signaling Technology, USA), anti-AKT, 1:1000 (No. 4691, Cell Signaling Technology, USA), anti-phospho-AKT, 1:1000 (No. 4051, Cell Signaling Technology, USA), and anti-GAPDH, 1:10,000 (No. 60004-1-Ig, Proteintech, USA).

Co-immunoprecipitation and immunohistochemistry

Co-immunoprecipitation and immunohistochemistry were performed as previously described [42, 43]·[9, 11]. The antibodies of co-immunoprecipitation are anti-TRPC1 (No. ACC-010, alomone labs, Israel) and anti-NCX1 (No. ANX-011, alomone labs, Israel). The GC and adjacent tissue microarray for immunostaining were purchased from SHANGHAI OUTDO BIOTECH CO., LTD (Shanghai, China). The tissue samples were incubated with anti-NCX1 (No. N216, Sigma, USA). The degree of staining in the NCX1 sections was observed and scored by two pathologists. According to previously defined criteria by T. Takenoue et al [44], the percentage of NCX1 positivity was scored from 0 to 3 as follows: 0, < 5%; 1, 5–25%; 2, 26–50%; 3, 51–75%;4, >=76%. The intensity of immunostaining was scored as: 0 (no staining); 1 (weak); 2 (moderate); and 3 (intense). Subsequently, the two scores were multiplied and the product was defined as immunohistochemical score. Accordingly, the final expression level of NCX1 was defined as low (0–4) and high (5–12). The IHC of mice tissue samples were incubated with anti-NCX1 (No. ANX-011, alomone labs, USA) and anti-Ki67 (No. ab15580, Abcam, UK).

Immunofluorescence assay

After fixed and blocked, the GC cells were incubated with anti-NCX1 antibody (No. MA3-926, Invitrogen) overnight at 4°C. Next, the cells were incubated with Cy3 labeled anti-mouse (No. A0521, Beyotime, China) secondary antibody for 1 h at room temperature. Then cells were incubated with anti-TRPC1 antibody (No. ACC-010, alomone labs, Israel) and 647 labeled anti-rabbit (No. A0468, Beyotime, China) secondary antibody for 1 h at room temperature respectively. Finally, nuclei were stained with DAPI for 5 min and images were captured using confocal microscope.

Cell proliferation and scratch assays

Cell proliferation assay was performed as previously described [9]. Cell proliferation was measured by CCK8 assay (No. C0038, Beyotime Biotechnology, China) according to the protocol of the manufacturer. Cell scratch assay was performed as previously described [45]. After scratching, gently wash the cell monolayer to remove detached cells. Then, replenish with serum free medium containing different drugs. 0 and 24 hours take photos respectively.

Transwell migration and invasion assays

Transwell migration and invasion assays were performed as previously described [9]. Cells were cultured upper chamber with 200 μL serum-free medium containing with different drugs. The lower chambers were filled with 600 μL medium plus 10% FBS. For invasion assays, the upper surface of the polycarbonate filter was coated with 10% Matrigel (Collaborative Biomedical, USA).

Measurement of $[Ca^{2+}]_{cyt}$ by digital Ca^{2+} imaging

$[Ca^{2+}]_{cyt}$ imaging experiments were performed as previously described [46, 47]. The PSS contained the following: 140 mM Na^+, 5 mM K^+, 2 mM Ca^{2+}, 147 mM Cl^-, 10 mM HEPES and 10 mM glucose (pH 7.4). The 0 Na^+ solution contained the following: 140 mM Li^+, 5 mM K^+, 2 mM Ca^{2+}, 147 mM Cl^-, 10 mM HEPES and 10 mM glucose (pH 7.4). The 0 Ca^{2+} solution contained the following: 140 mM Na^+, 5 mM K^+, 145 mM Cl^-, 0.5 mM EGTA, 10 mM HEPES and 10 mM glucose (pH 7.4). The 0 Na^+-0 Ca^{2+} solution contained the following: 140 mM Li^+, 5 mM K^+, 145 mM Cl^-, 0.5 mM EGTA, 10 mM HEPES and 10 mM glucose (pH 7.4).

Tumor xenograft and peritoneal dissemination assays in nude mice

Tumor xenograft assay was performed as previously described [11]. After tumor sizes grow to 1 mm^3, $CaCl_2$ (4 mM), KB-R7943 (30 μM), or $CaCl_2$ plus KB-R7943 were injected into the tumors in one side of the armpits once a day, and 0.1% DMSO into the other side as controls. Similarly, the shNCX1 SGC7901 cells or negative control NC was separately injected into each side, and $CaCl_2$ was injected into the tumors of each side once a day. Four weeks later, xenografted tumors were quantified. For the peritoneal dissemination assay, 1×10^6 shNCX1 SGC7901 cells and the NC cells were injected into the abdominal cavity of nude mice. $CaCl_2$ (4 mM) was injected into abdominal cavity once a day. Five weeks later, xenografted tumors were quantified.

Statistical analysis

SPSS Statistics 26.0 (RRID:SCR_002865, USA) and GraphPad Prism 7.0 (RRID:SCR_002798, USA) software were used to analyze the data. All data shown are means ± SD. All experiments were at least three biological repeated. Student's unpaired, two-tailed t test or one-way ANOVA were used to analyze statistical significance differences of experimental groups. The patient survival was examined by the log-rank test using the *Kaplan-Meier* method. Significant differences (*$P < 0.05$) are expressed in the figures and figure legends.

Declarations

Acknowledgements

These studies were supported by research grants from the National Natural Science Foundation of China (No. 81972328 to HXW, No. 81873544 to HD, and No. 82103591 to NNG).

Conflict of Interest: The authors declare that they have no competing interests.

Authors' contributions

Hui Dong conceived the study, designed and supervised the experiments, wrote, revised and finalized the manuscript. Hanxing Wan designed some experiments, performed most experiments and data

analysis, and wrote the draft. Nannan Gao performed most experiments and data analysis. Wei Lu, Chen Lu and Jun Chen performed some experiments. All authors reviewed the manuscript and declare that they have no competing interests.

References

1. Joshi SS, Badgwell BD. Current treatment and recent progress in gastric cancer. CA Cancer J Clin 2021; 71: 264–279.
2. Seo JH, Fox JG, Peek RM, Jr., Hagen SJ. N-methyl D-aspartate channels link ammonia and epithelial cell death mechanisms in Helicobacter pylori Infection. Gastroenterology 2011; 141: 2064–2075.
3. Chen J, Sitsel A, Benoy V, Sepulveda MR, Vangheluwe P. Primary Active Ca(2+) Transport Systems in Health and Disease. Cold Spring Harb Perspect Biol 2020; 12.
4. Patergnani S, Danese A, Bouhamida E, Aguiari G, Previati M, Pinton P *et al*. Various Aspects of Calcium Signaling in the Regulation of Apoptosis, Autophagy, Cell Proliferation, and Cancer. Int J Mol Sci 2020; 21.
5. Berridge MJ. The Inositol Trisphosphate/Calcium Signaling Pathway in Health and Disease. Physiol Rev 2016; 96: 1261–1296.
6. Marchi S, Giorgi C, Galluzzi L, Pinton P. Ca(2+) Fluxes and Cancer. Mol Cell 2020; 78: 1055–1069.
7. Monteith GR, Prevarskaya N, Roberts-Thomson SJ. The calcium-cancer signalling nexus. Nat Rev Cancer 2017; 17: 367–380.
8. Monteith GR, McAndrew D, Faddy HM, Roberts-Thomson SJ. Calcium and cancer: targeting Ca2 + transport. Nat Rev Cancer 2007; 7: 519–530.
9. Gao N, Yang F, Chen S, Wan H, Zhao X, Dong H. The role of TRPV1 ion channels in the suppression of gastric cancer development. J Exp Clin Cancer Res 2020; 39: 206.
10. Tang B, Wu J, Zhu MX, Sun X, Liu J, Xie R *et al*. VPAC1 couples with TRPV4 channel to promote calcium-dependent gastric cancer progression via a novel autocrine mechanism. Oncogene 2019; 38: 3946–3961.
11. Xie R, Xu J, Xiao Y, Wu J, Wan H, Tang B *et al*. Calcium Promotes Human Gastric Cancer via a Novel Coupling of Calcium-Sensing Receptor and TRPV4 Channel. Cancer Res 2017; 77: 6499–6512.
12. Ottolia M, Philipson KD. NCX1: mechanism of transport. Adv Exp Med Biol 2013; 961: 49–54.
13. Blaustein MP, Lederer WJ. Sodium/calcium exchange: its physiological implications. Physiol Rev 1999; 79: 763–854.
14. Chovancova B, Liskova V, Babula P, Krizanova O. Role of Sodium/Calcium Exchangers in Tumors. Biomolecules 2020; 10.
15. Rodrigues T, Estevez GNN, Tersariol I. Na(+)/Ca(2+) exchangers: Unexploited opportunities for cancer therapy? Biochem Pharmacol 2019; 163: 357–361.
16. Zhang F, Wan H, Chu F, Lu C, Chen J, Dong H. Small intestinal glucose and sodium absorption through calcium-induced calcium release and store-operated Ca(2+) entry mechanisms. Br J

Pharmacol 2021; 178: 346–362.

17. Kemeny LV, Schnur A, Czepan M, Rakonczay Z, Jr., Gal E, Lonovics J *et al*. Na+/Ca2 + exchangers regulate the migration and proliferation of human gastric myofibroblasts. Am J Physiol Gastrointest Liver Physiol 2013; 305: G552-563.
18. Wen J, Pang Y, Zhou T, Qi X, Zhao M, Xuan B *et al*. Essential role of Na+/Ca2 + exchanger 1 in smoking-induced growth and migration of esophageal squamous cell carcinoma. Oncotarget 2016; 7: 63816–63828.
19. Xu J, Yang Y, Xie R, Liu J, Nie X, An J *et al*. The NCX1/TRPC6 Complex Mediates TGFbeta-Driven Migration and Invasion of Human Hepatocellular Carcinoma Cells. Cancer Res 2018; 78: 2564–2576.
20. Timmons JA, Rao JN, Turner DJ, Zou T, Liu L, Xiao L *et al*. Induced expression of STIM1 sensitizes intestinal epithelial cells to apoptosis by modulating store-operated Ca2 + influx. J Gastrointest Surg 2012; 16: 1397–1405.
21. Elzamzamy OM, Penner R, Hazlehurst LA. The Role of TRPC1 in Modulating Cancer Progression. Cells 2020; 9.
22. Davis FM, Peters AA, Grice DM, Cabot PJ, Parat MO, Roberts-Thomson SJ *et al*. Non-stimulated, agonist-stimulated and store-operated Ca2 + influx in MDA-MB-468 breast cancer cells and the effect of EGF-induced EMT on calcium entry. PLoS One 2012; 7: e36923.
23. Dong H, Shim KN, Li JM, Estrema C, Ornelas TA, Nguyen F *et al*. Molecular mechanisms underlying Ca2+-mediated motility of human pancreatic duct cells. Am J Physiol Cell Physiol 2010; 299: C1493-1503.
24. Zhang Z, Ren L, Zhao Q, Lu G, Ren M, Lu X *et al*. TRPC1 exacerbate metastasis in gastric cancer via ciRS-7/miR-135a-5p/TRPC1 axis. Biochem Biophys Res Commun 2020; 529: 85–90.
25. Ge P, Wei L, Zhang M, Hu B, Wang K, Li Y *et al*. TRPC1/3/6 inhibition attenuates the TGF-beta1-induced epithelial-mesenchymal transition in gastric cancer via the Ras/Raf1/ERK signaling pathway. Cell Biol Int 2018; 42: 975–984.
26. Long Y, Wang WP, Yuan H, Ma SP, Feng N, Wang L *et al*. Functional comparison of the reverse mode of Na+/Ca2 + exchangers NCX1.1 and NCX1.5 expressed in CHO cells. Acta Pharmacol Sin 2013; 34: 691–698.
27. Harper AG, Sage SO. TRP-Na(+)/Ca(2+) Exchanger Coupling. Adv Exp Med Biol 2016; 898: 67–85.
28. Wang H, Deng G, Ai M, Xu Z, Mou T, Yu J *et al*. Hsp90ab1 stabilizes LRP5 to promote epithelial-mesenchymal transition via activating of AKT and Wnt/beta-catenin signaling pathways in gastric cancer progression. Oncogene 2019; 38: 1489–1507.
29. Zhao J, Ou B, Han D, Wang P, Zong Y, Zhu C *et al*. Tumor-derived CXCL5 promotes human colorectal cancer metastasis through activation of the ERK/Elk-1/Snail and AKT/GSK3beta/beta-catenin pathways. Mol Cancer 2017; 16: 70.
30. Fujimoto Y, Hayashi S, Azuma YT, Mukai K, Nishiyama K, Kita S *et al*. Overexpression of Na(+)/Ca(2+) exchanger 1 display enhanced relaxation in the gastric fundus. J Pharmacol Sci 2016; 132: 181–186.

31. Dong H, Tang B, Jiang Y, Mittal RK. Na(+) /Ca(2+) exchanger 1 is a key mechanosensitive molecule of the esophageal myenteric neurons. Acta Physiol (Oxf) 2019; 225: e13223.
32. Dong H, Sellers ZM, Smith A, Chow JY, Barrett KE. Na(+)/Ca(2+) exchange regulates Ca(2+)-dependent duodenal mucosal ion transport and HCO(3)(-) secretion in mice. Am J Physiol Gastrointest Liver Physiol 2005; 288: G457-465.
33. Tang B, Chow JY, Dong TX, Yang SM, Lu DS, Carethers JM *et al*. Calcium sensing receptor suppresses human pancreatic tumorigenesis through a novel NCX1/Ca(2+)/beta-catenin signaling pathway. Cancer Lett 2016; 377: 44–54.
34. Mahdi SH, Cheng H, Li J, Feng R. The effect of TGF-beta-induced epithelial-mesenchymal transition on the expression of intracellular calcium-handling proteins in T47D and MCF-7 human breast cancer cells. Arch Biochem Biophys 2015; 583: 18–26.
35. Hu HJ, Wang SS, Wang YX, Liu Y, Feng XM, Shen Y *et al*. Blockade of the forward Na(+) /Ca(2+) exchanger suppresses the growth of glioblastoma cells through Ca(2+) -mediated cell death. Br J Pharmacol 2019; 176: 2691–2707.
36. Liu Z, Cheng Q, Ma X, Song M. Suppressing Effect of Na(+)/Ca(2+) Exchanger (NCX) Inhibitors on the Growth of Melanoma Cells. Int J Mol Sci 2022; 23.
37. Wessler S, Krisch LM, Elmer DP, Aberger F. From inflammation to gastric cancer - the importance of Hedgehog/GLI signaling in Helicobacter pylori-induced chronic inflammatory and neoplastic diseases. Cell Commun Signal 2017; 15: 15.
38. Iimuro M, Nakamura S, Arakawa T, Wakabayashi K, Mutoh M. Effects of dietary calcium on Helicobacter pylori-induced gastritis in Mongolian gerbils. Anticancer Res 2013; 33: 3667–3674.
39. Ghanayem BI, Matthews HB, Maronpot RR. Calcium channel blockers protect against ethanol- and indomethacin-induced gastric lesions in rats. Gastroenterology 1987; 92: 106–111.
40. Tatsuta M, Iishi H, Baba M, Nakaizumi A, Uehara H, Taniguchi H. Effect of calcium channel blockers on gastric carcinogenesis and caerulein enhancement of gastric carcinogenesis induced by N-methyl-N'-nitro-N-nitrosoguanidine in Wistar rats. Cancer Res 1990; 50: 2095–2098.
41. Percie du Sert N, Hurst V, Ahluwalia A, Alam S, Avey MT, Baker M *et al*. The ARRIVE guidelines 2.0: Updated guidelines for reporting animal research. Br J Pharmacol 2020; 177: 3617–3624.
42. Xu J, Ji B, Wen G, Yang Y, Jin H, Liu X *et al*. Na+/H + exchanger 1, Na+/Ca2 + exchanger 1 and calmodulin complex regulates interleukin 6-mediated cellular behavior of human hepatocellular carcinoma. Carcinogenesis 2016; 37: 290–300.
43. Wang F, Zhang J, Tang H, Pang Y, Ke X, Peng W *et al*. Nup54-induced CARM1 nuclear importation promotes gastric cancer cell proliferation and tumorigenesis through transcriptional activation and methylation of Notch2. Oncogene 2022; 41: 246–259.
44. Takenoue T, Kitayama J, Takei Y, Umetani N, Matsuda K, Nita ME *et al*. Characterization of dihydropyrimidine dehydrogenase on immunohistochemistry in colon carcinoma, and correlation between immunohistochemical score and protein level or messenger RNA expression. Ann Oncol 2000; 11: 273–279.

45. Martinotti S, Ranzato E. Scratch Wound Healing Assay. Methods Mol Biol 2020; 2109: 225–229.
46. Zhang F, Wan H, Yang X, He J, Lu C, Yang S *et al*. Molecular mechanisms of caffeine-mediated intestinal epithelial ion transports. Br J Pharmacol 2019; 176: 1700–1716.
47. Wan H, Xie R, Xu J, He J, Tang B, Liu Q *et al*. Anti-proliferative Effects of Nucleotides on Gastric Cancer via a Novel P2Y6/SOCE/Ca(2+)/beta-catenin Pathway. Sci Rep 2017; 7: 2459.

Figures

Figure 1.

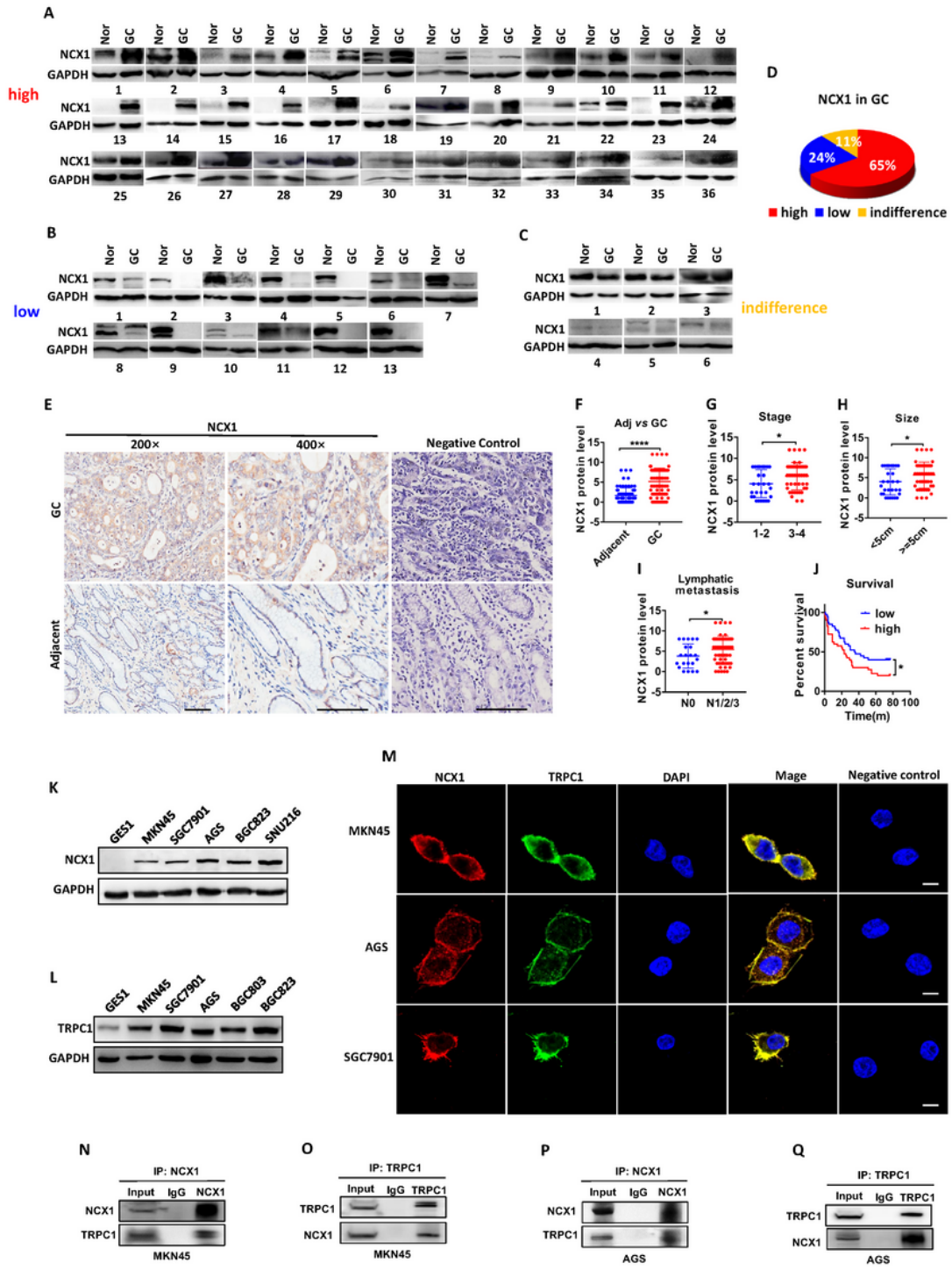

Figure 1

The enhanced expression of NCX1 and TRPC1 in human primary gastric cancer tissues and cells

(A-C) Western blot analysis applied to compare the expression levels of NCX1 proteins between gastric cancer (GC) tissues and adjacent normal (Nor) tissues from 55 GC patients: 36 pairs with high expression (A), 13 pairs with low expression (B), and 6 pairs without difference (C). **(D)** Summary data showing the

percentage of high, low and indifference of NCX1 expression in GC tissues compared to adjacent tissues. **(E-F)** Representative and summary data of immunohistological staining on NCX1 proteins in GC tissues compared to adjacent tissues. Scale bar = 100 μm for each image. Negative control: without primary antibody. (****$P < 0.0001$, n = 80 patients). **(G-I)** Relative NCX1 protein levels in GC tissues from the patients with different stages (G), tumor sizes (H), and lymphatic metastasis (I). (*$P < 0.05$, n = 80 patients). **(J)** Kaplan–Meier analysis of survival ratio of GC patients with low and high NCX1 expression levels (*$P < 0.05$, n = 80 patients). **(K-I)** Western blot analysis of NCX1 and TRPC1 protein levels in GES1 and GC cell lines. **(M)** Immunofluoresence staining images of NCX1 and TRPC1 proteins with primary antibody and without the antibody (negative control) in MKN45, AGS and SGC7901 cells. Scale bar = 10 μm for each image. **(N-Q)** Co-immunoprecipitation showing the binding of NCX1 and TRPC1 proteins in GC cells.

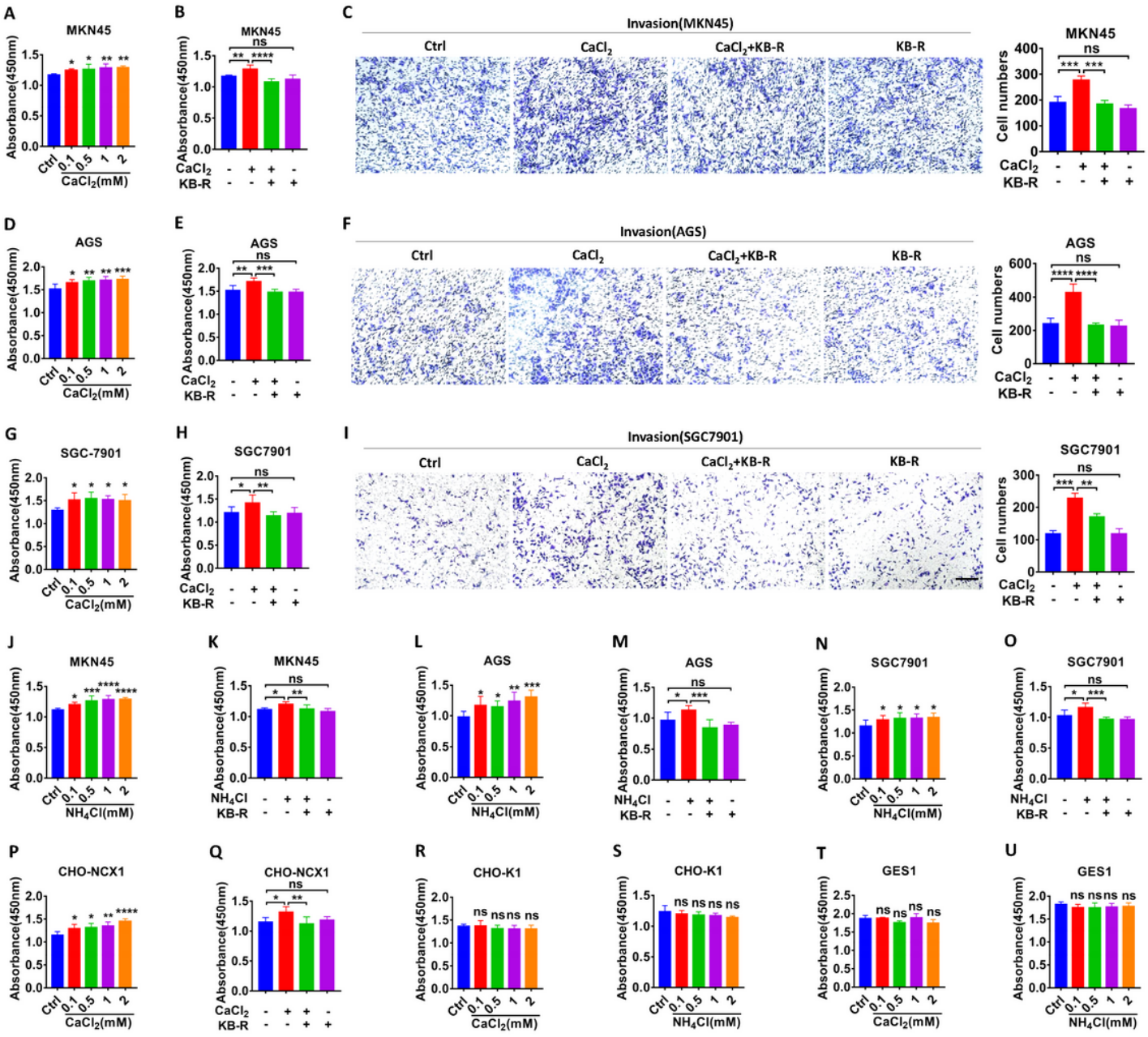

Figure 2

NCX1 activation promotes proliferation and invasion of human GC cells

(A, D, G) Dose-dependently enhanced proliferation of $CaCl_2$ (0.1-2 mM) in MKN45 (A), AGS (D), and SGC7901 (G) cells. **(B-C, E-F, H-I)** The inhibitory effect of KB-R7943 (KB-R, 1 μM in MKN45, 4 μM in AGS, 8 μM in SGC7901) on $CaCl_2$ (1mM)-induced proliferation (B, E, H) and invasion (C, F, I) of GC cells, Scale bar = 200 μm for each image. **(J-O)**. Dose-dependently enhanced proliferation of NH_4Cl (0.1-2 mM) in MKN45

(J), AGS (L), and SGC7901 (N) cells, and the inhibitory effect of KB-R7943 on NH_4Cl (1 mM)-induced proliferation of MKN45 (K), AGS (M), and SGC7901 (O) cells. **(P, Q)** Dose-dependently enhanced proliferation of $CaCl_2$ (0.1-2 mM) in CHO-NCX1 with NCX1 overexpression, and the inhibitory effect of KB-R7943 (0.2 μM) on $CaCl_2$ (1 mM)-induced proliferation of CHO-NCX1 cells. **(R-U)** No effects of $CaCl_2$ (0.1-2 mM) and NH_4Cl (0.1-2 mM) on proliferation of CHO-K1 without NCX1 overexpression and GES cells. (*P < 0.05, **P < 0.01, ***P < 0.001, ****P < 0.0001, n = 3; ns, no significant differences).

Figure 3.

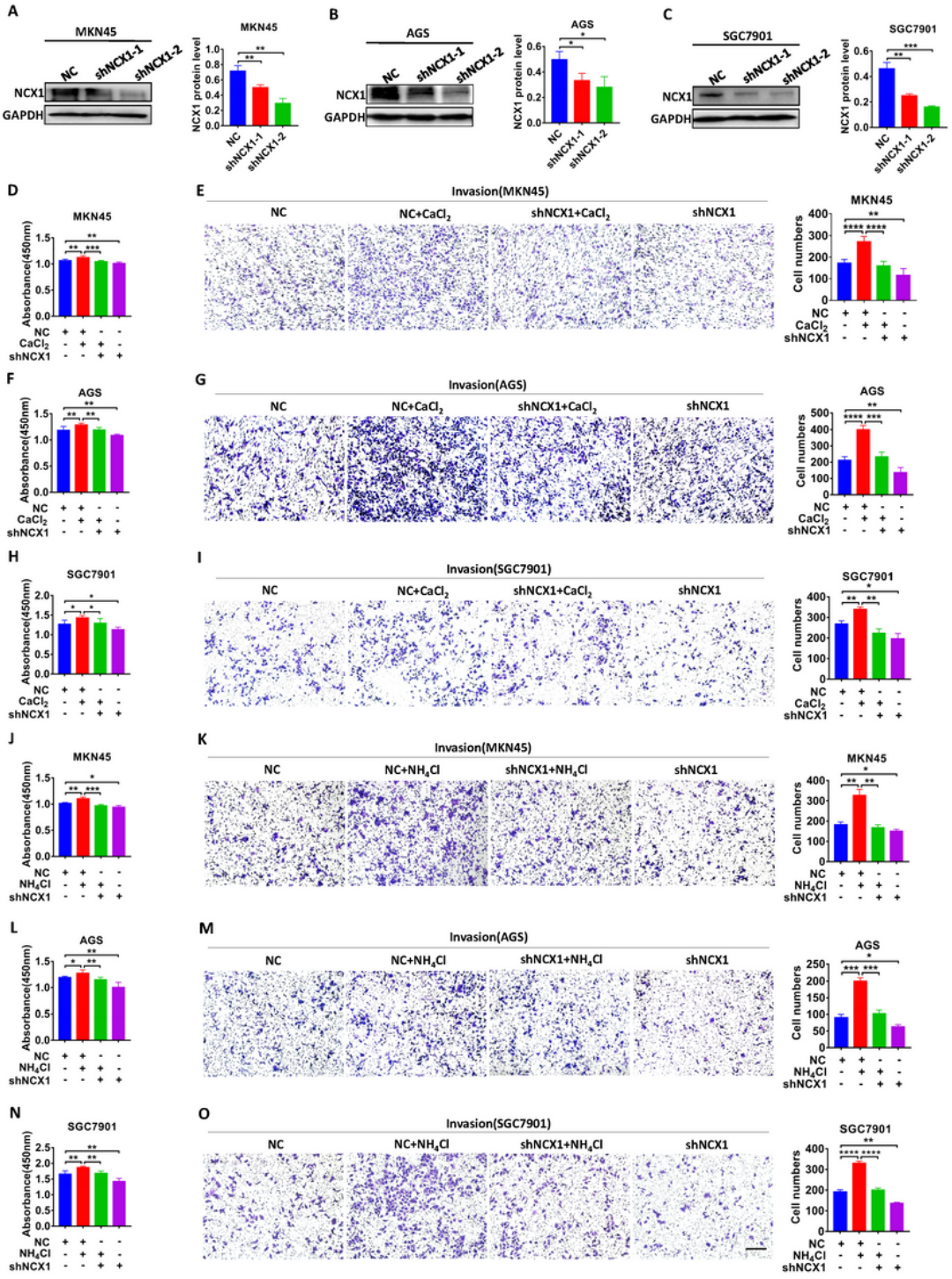

Figure 3

$CaCl_2$ and NH_4Cl promote proliferation and invasion of human GC cells through NCX1 activation

(A-C) Representative images of NCX1 protein expression in GC cells with NCX1 knockdown and summary data of NCX1 protein levels in MKN45 (A), AGS (B), and SGC7901 (C) cells (*P < 0.05, **P < 0.01, ***P < 0.001, *vs*. NC, n = 3). **(D-E, F-G, H-I)** The effect of shNCX1 on $CaCl_2$ (1 mM)-induced proliferation (D, F, H) and invasion (E, G, I) of GC cells. **(J-K, L-M, N-O)** The effect of shNCX1 on NH_4Cl (1 mM)-induced proliferation (J, L, N) and invasion (K, M, O) of GC cells. Scale bar = 200 μm for each image. (*P < 0.05, **P < 0.01, ***P < 0.001, ****P < 0.0001, n = 3; ns, no significant differences).

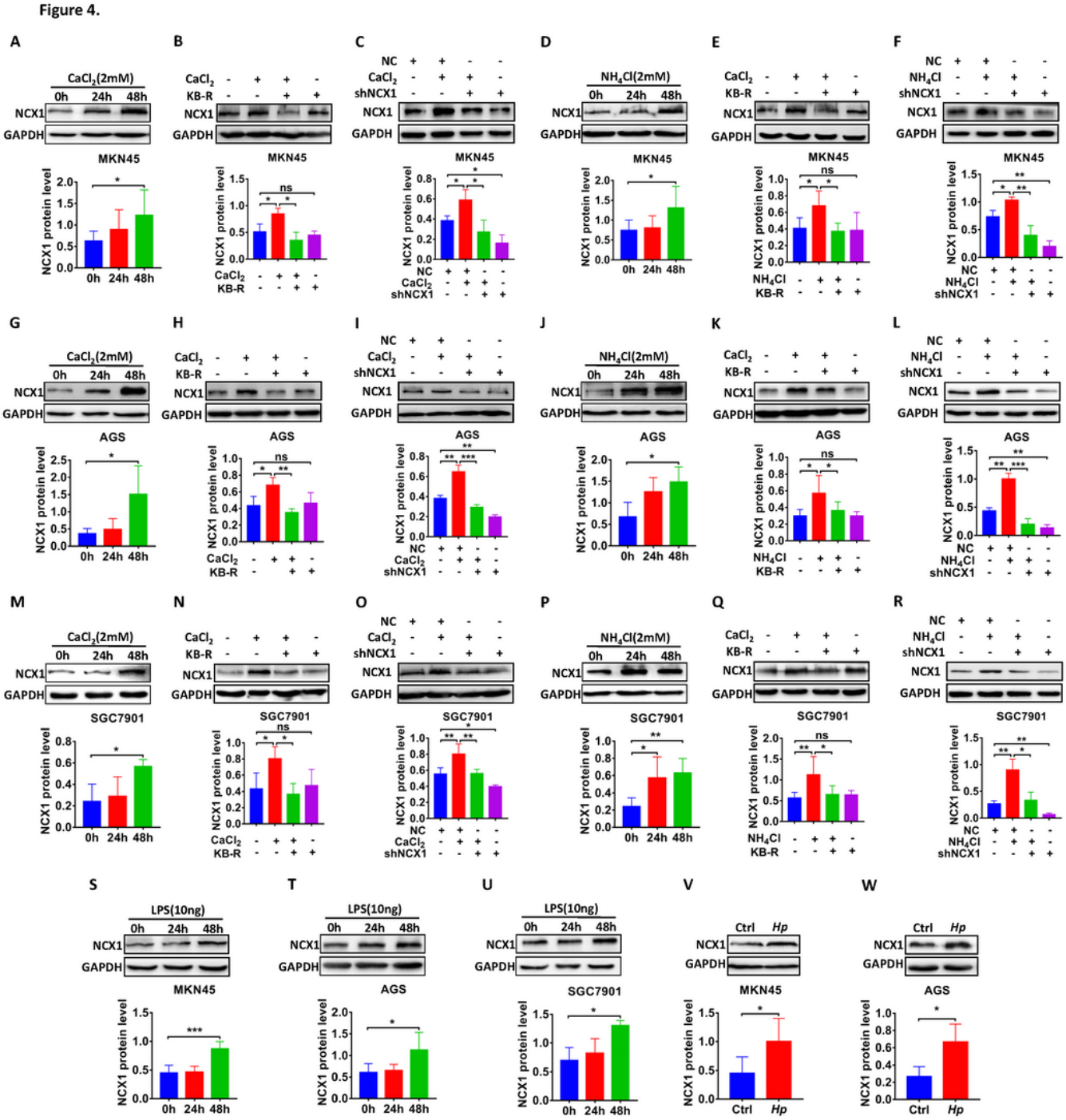

Figure 4

$CaCl_2$, *Hp* and virulence factors enhance NCX1 expression in human GC cells

(A, G, M) Representative time courses of $CaCl_2$ (2 mM)-enhanced NCX1 protein expression in GC cells. **(B-C, H-I, N-O)** Inhibitory effect of KB-R7943 (KB-R, 1 μM in MKN45, 4 μM in AGS, 8 μM in SGC7901) (B, H, N) or shNCX1 (C, I, O) on $CaCl_2$ (2 mM)-enhanced NCX1 expression in GC cells. **(D, J, P)** Representative time

courses of NH_4Cl (2 mM)-enhanced NCX1 protein expression in GC cells. **(E-F, K-L, Q-R)** Inhibitory effect of KB-R7943 (E, K, Q) or shNCX1 (F, L, R) on NH_4Cl (2 mM)-enhanced NCX1 protein expression in GC cells. **(S, T, U)** Representative time courses LPS (10 ng)-enhanced NCX1 protein expression in GC cells. **(V, W)** Representative time courses *H. pylori*-enhanced NCX1 protein in GC cells. (**P* < 0.05, ***P* < 0.01, ****P* < 0.001, n = 3; ns, no significant differences).

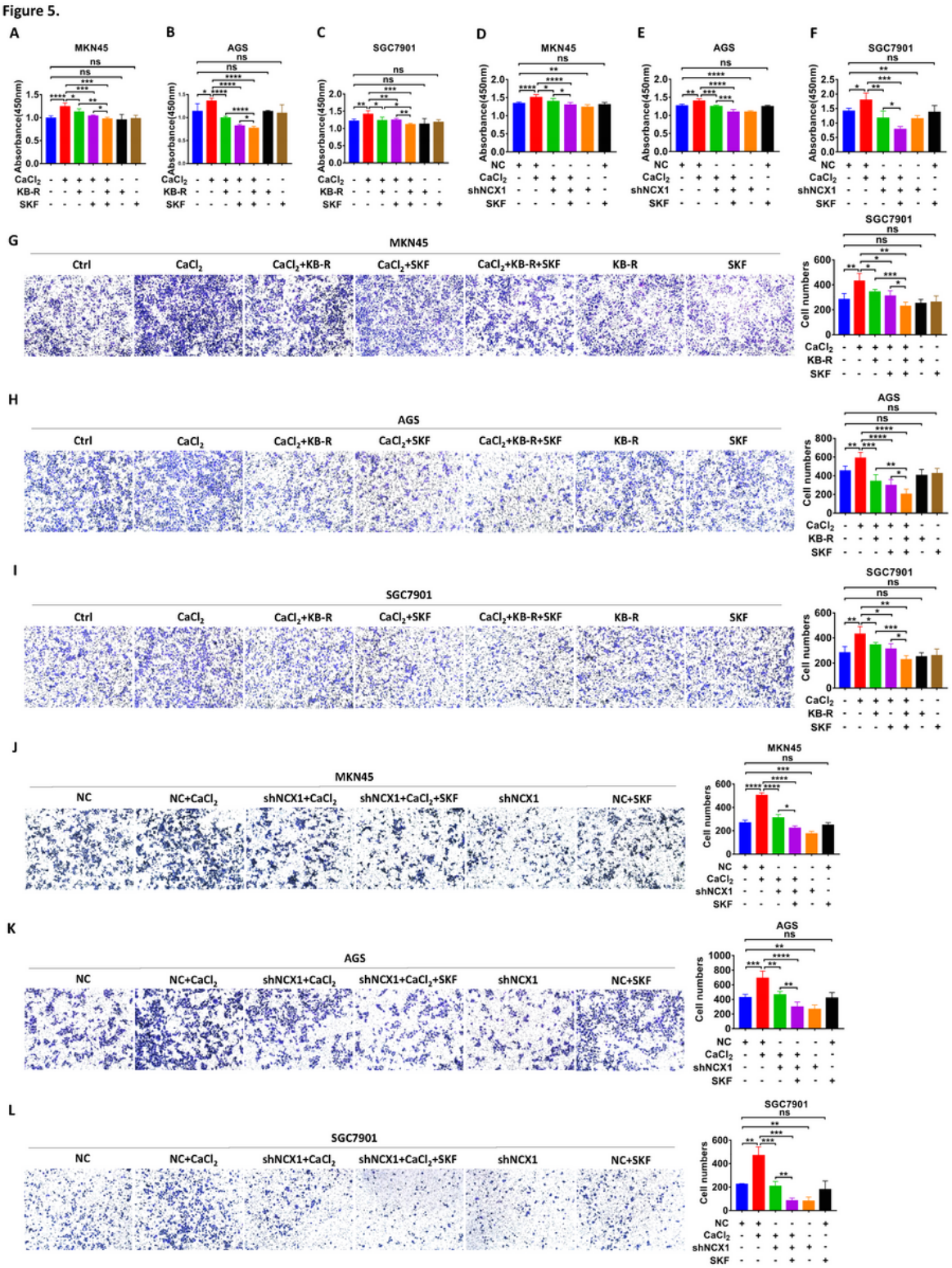

Figure 5

NCX1 coordinates with TRPC1 to promote proliferation and migration of human GC cells

(A-C, G-I) Summary data showing the inhibitory effects of either KB-R7943 (KB-R, 1 μM in MKN45, 4 μM in AGS, 8 μM in SGC7901), SKF96365 (SKF, 1 μM) or KB-R plus SKF on $CaCl_2$ (1 mM)-enhanced proliferation (A-C) and migration (G-I) of GC cells. **(D-F, J-L)** Summary data showing the inhibitory effect of either shNCX1, SKF96365 (SKF, 1 μM) or shNCX1 plus SKF on $CaCl_2$ (1 mM)-enhanced proliferation (D-F) and migration (J-L) of GC cells. Scale bar = 200 μm for each image. (**P* < 0.05, ***P* < 0.01, ****P* < 0.001, *****P* < 0.0001, n = 3; ns, no significant differences).

Figure 6.

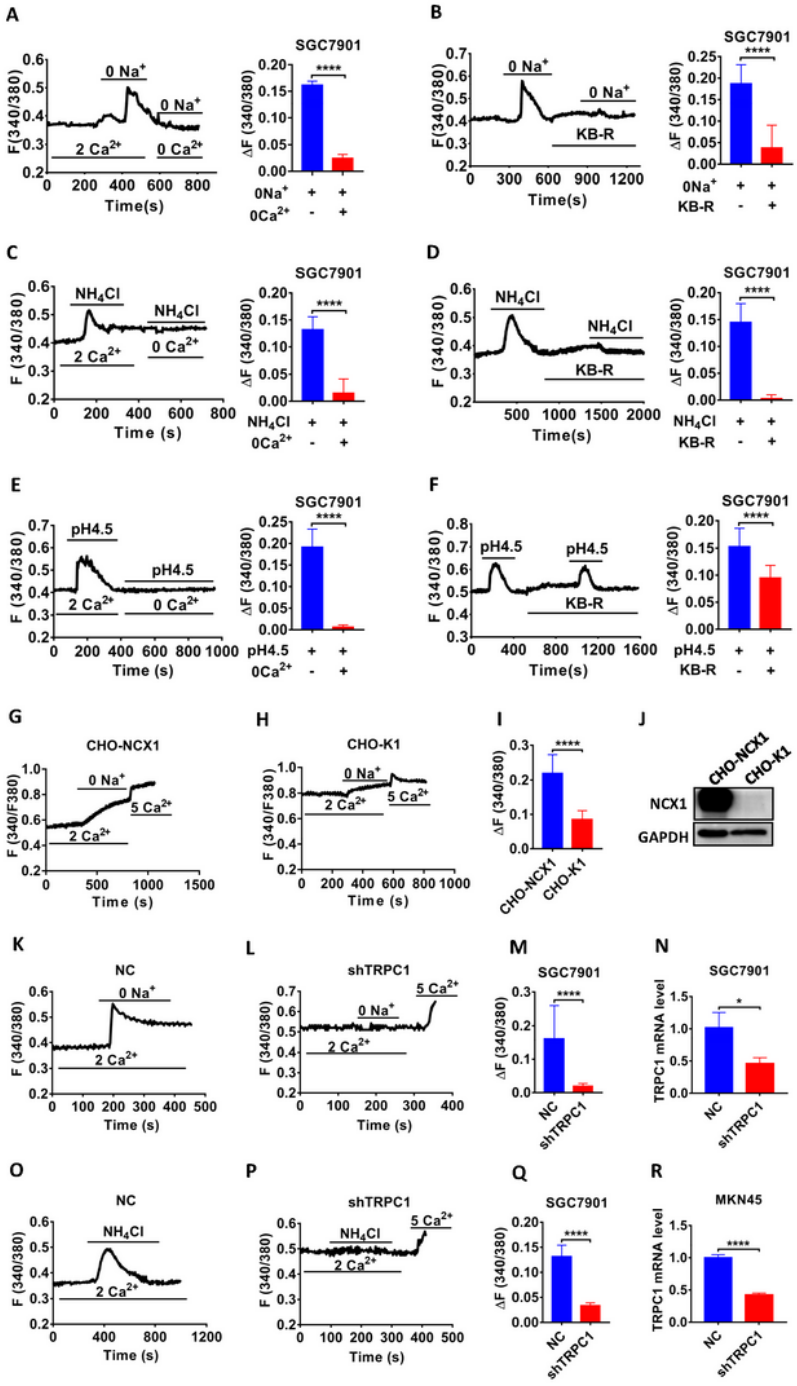

Figure 6

Hp virulence factor and acid stimulate NCX1/TRPC1 coupling in human GC cells

(A, C, E) Summary tracings of $[Ca^{2+}]_{cyt}$ time courses in response to extracellular 0 Na^+ (A), NH_4Cl (5 mM) (C) and pH 4.5 (E) in the presence of extracellular 2 Ca^{2+} or 0 Ca^{2+} (left). Summary data showing the peaks of 0 Na^+, NH_4Cl and pH 4.5-increased $[Ca^{2+}]_{cyt}$ signaling in SGC7901 cells (right) (A, n = 20 cells; C,

n = 11 cells; E, n = 11 cells, ****$P < 0.0001$). **(B, D, F)** Summary tracings of $[Ca^{2+}]_{cyt}$ time courses in response to 0 Na^+ (B), NH_4Cl (5 mM) (D) and pH4.5 (F) in the presence of 2 Ca^{2+} or 2 Ca^{2+} plus KB-R7943 (KB-R, 30 μM) (left). Summary data showing the peaks of 0 Na^+, NH_4Cl and pH 4.5-increased $[Ca^{2+}]_{cyt}$ signaling in SGC7901 cells (right) (B, n = 20 cells; D, n = 23 cells; F, n = 26 cells, ****$P < 0.0001$). **(G, H)** Summary tracings of $[Ca^{2+}]_{cyt}$ time courses in response to 0 Na^+ in the presence of 2 Ca^{2+} or 5Ca^{2+} in CHO-NCX1 (G) and CHO-K1 (H) cells. **(I)** Summary data showing the peaks of 0 Na^+-increased $[Ca^{2+}]_{cyt}$ signaling described as in G-H (G, n = 23 cells; H, n = 17 cells, ****$P < 0.0001$). **(J)** Western blot analysis of NCX1 protein levels in CHO-NCX1 and CHO-K1 cells. **(K-L, O-P)** Summary tracings of $[Ca^{2+}]_{cyt}$ time courses in response to 0 Na^+ (K-L) and NH_4Cl (5mM) (O-P) in the presence of 2 Ca^{2+} in NC (K, O) or shTRPC1 (L, P) of SGC7901 cells. **(M, Q)** Summary data showing the peaks of 0 Na^+ (M) or NH_4Cl (Q)-increased $[Ca^{2+}]_{cyt}$ signaling described as in K-L, O-P (n = 11 cells, ****$P < 0.0001$). **(N, R)** RT-PCR analysis of TRPC1 mRNA levels in NC and shTRPC1 of GC cells (n = 3, *$P < 0.05$, ****$P < 0.0001$). Each one is 3 independent experiments with similar results.

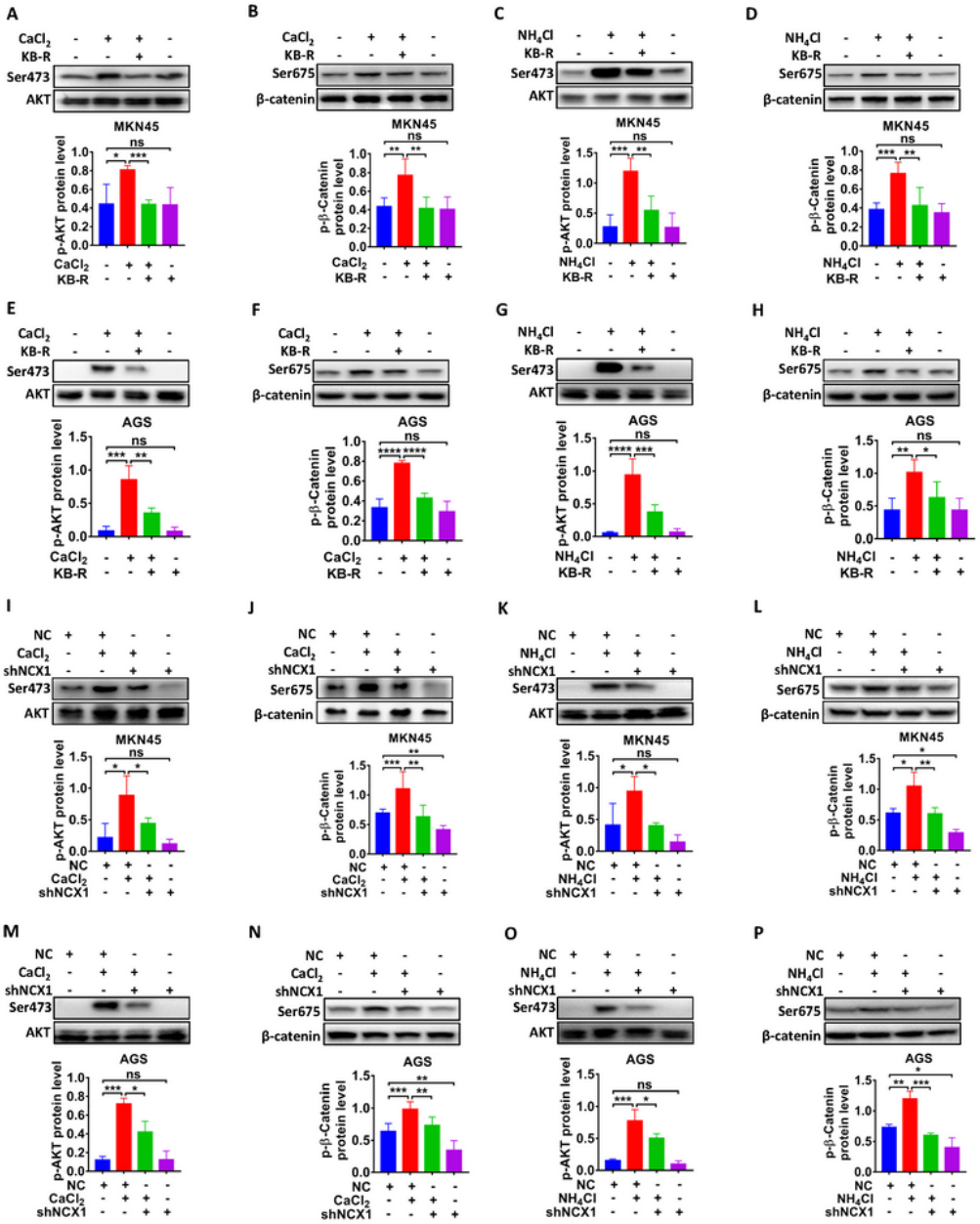

Figure 7

NCX1 activation induces phosphorylation of AKT and β-catenin in human GC cells

(A-B, E-F) Inhibitory effect of KB-R7943 (KB-R, 1 μM in MKN45, 4 μM in AGS) on $CaCl_2$ (2 mM)-induced AKT and β-catenin phosphorylation in MKN45 and AGS cells. **(C-D, G-H)** Inhibitory effect of KB-R7943 on NH_4Cl (2 mM)-induced AKT and β-catenin phosphorylation in MKN45 and AGS cells. **(I-J, M-N)** Inhibitory

effect of shNCX1 on $CaCl_2$-induced AKT and β-catenin phosphorylation in MKN45 and AGS cells. **(K-L, O-P)** Inhibitory effect of shNCX1 on NH_4Cl-induced AKT and β-catenin phosphorylation in MKN45 and AGS cells. (*P < 0.05, **P < 0.01, ***P < 0.001, ****P < 0.0001, n = 3; ns, no significant differences).

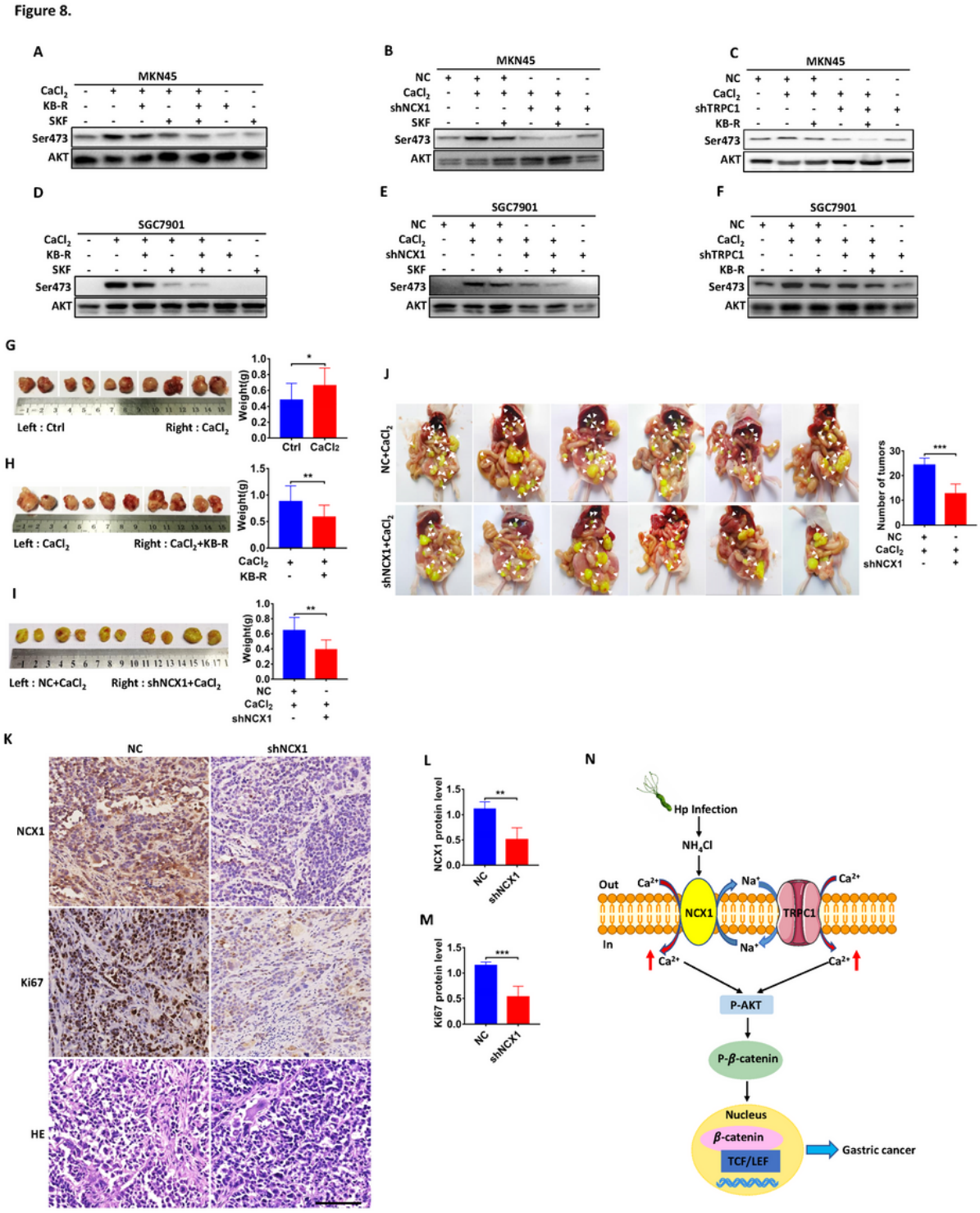

Figure 8

TRPC1/NCX1 coupling induces AKT phosphorylation and promotes GC growth and metastasis

(A, D) Inhibitory effects of either KB-R7943 (KB-R, 1 μM in MKN45, 8 μM in SGC7901), SKF96365 (SKF, 1 μM) or KB-R plus SKF on $CaCl_2$ (2 mM)-induced AKT phosphorylation in GC cells. **(B, E)** Inhibitory effects of SKF, shNCX1 or shNCX1 plus SKF on $CaCl_2$ (2 mM)-induced AKT phosphorylation in GC cells. **(C, F)** Inhibitory effects of either KB-R, shTRPC1 or shTRPC1 plus KB-R on $CaCl_2$-induced AKT phosphorylation in GC cells. **(G, H, I)** $CaCl_2$ promoted growth of xenografted gastric tumors (G), which was attenuated by either KB-R7943 (H) or shNCX1 (I). **(J)** Inhibitory effects of shNCX1 on $CaCl_2$-induced gastric tumor metastasis. **(K)** Immunohistochemical analysis and histological examination on expression of NCX1 and Ki67 proteins with or without NCX1 knockdown in GC tissues. Scale bar=100 μm for each image. **(L, M)** Summary data comparing expression of NCX1 and Ki67 proteins analyzed by immunohistochemistry between with or without NCX1 knockdown in GC tissues. (*P < 0.05, **P < 0.01, ***P < 0.001, ****P < 0.0001, n = 3; ns, no significant differences). **(N)** The proposed oncogenic mechanisms of TRPC1/NCX1 coupling via Ca^{2+}/AKT/β-catenin pathway in *Hp*-associated GC.

Supplementary Files

This is a list of supplementary files associated with this preprint. Click to download.

- Supplementaryfigure.pdf
- Supplementarytable1.doc